Polymorphs of Alumina Predicted by First Principles: Putting Pressure on the Ruby Pressure Scale

Kendall T. Thomson,* Renata M. Wentzcovitch,
Mark S. T. Bukowinski

Fully optimized quantum mechanical calculations indicate that Al_2O_3 transforms from the corundum structure to the as yet unobserved Rh_2O_3 (II) structure at about 78 gigapascals, and it further transforms to *Pbnm*-perovskite structure at 223 gigapascals. The predicted x-ray spectrum of the Rh_2O_3 (II) structure is similar to that of the corundum structure, suggesting that the Rh_2O_3 (II) structure could go undetected in high-pressure x-ray measurements. It is therefore possible that the ruby (Cr^{3+}-doped corundum) fluorescence pressure scale is sensitive to the thermal history of the ruby chips in a given experiment.

Corundum (Al_2O_3 with an α-alumina structure), besides being a model ceramic material (*1*), has important applications in high-pressure research. It is used as a window material in shock wave experiments (*2*) and, when doped with Cr^{3+} (ruby), the pressure dependent shift in its flourescence line serves as the pressure calibrant (the ruby scale) in diamond-anvil cell measurements (*3, 4*). The ruby scale has been calibrated up to 180 GPa (*5*) and pressures as high as 550 GPa have been inferred by linear extrapolation of the scale at about 298 K (*4*). No phase transformation has been observed in experimental studies up to a pressure of 175 GPa, suggesting that corundum is the stable phase up to this pressure (*4, 6*). However, previous computational studies of Al_2O_3 utilizing ionic models (*7–9*) have suggested that phase transformations may occur at high pressures. The predicted transformation pressures (between 6 and 148 GPa) were poorly constrained (*7–9*), but a recent linearized, augmented plane-wave (LAPW) calculation (*10*) predicted that corundum transforms to a Rh_2O_3 (II) structure of Al_2O_3 [hereafter referred to as Rh_2O_3 (II)] at about 90 GPa.

We used a plane-wave basis set (*11*) and norm-conserving pseudopotentials (*12*) with an ab initio algorithm capable of fully optimizing complex structural geometries at arbitrary pressures and 0 K (*12*) to investigate further this transition and other possible phase transformations in Al_2O_3 at high pressures. We were particularly interested in considering the effects of structural relaxation, which was not considered in (*10*), on the location of any possible phase transition pressures calculated for Al_2O_3. Our algorithm combines a fully quantum mechanical method—within the local density approximation (LDA) (*13, 14*) to density functional theory—with an efficient structural optimization strategy derived from a variable cell shape molecular dynamics technique (*15, 16*). The reliability of the LDA to predict correct structural energetics and transition pressures was demonstrated on the high-pressure phases of silicon (*17*) and, since then, in other solids (*16, 18*). The recent introduction of a variable cell shape in these calculations (*16*) enables finite temperature, constant pressure molecular dynamics simulations, as well as optimization of structures with large numbers of degrees of freedom at arbitrary pressures. This type of optimization has broadened the spectrum of phases tractable by the first principles technique and has allowed unbiased searches in parameter spaces of arbitrary dimensions.

We investigated four candidate structures: corundum, Rh_2O_3 (II), *Pbnm*-perovskite, and $R\bar{3}c$-perovskite, up to 450 GPa. The likelihood that corundum transforms to a Rh_2O_3 (II) polymorph stems from a similarly observed structural transformation of rhodium sesquioxide (*19*). Both structures exhibit Al octahedrally coordinated to oxygen with edge-sharing AlO_6 polyhedra. The difference is in the number of shared edges each polyhedra has—three in the case of corundum and two for Rh_2O_3 (II) (Fig. 1, A and B). The Rh_2O_3 (II) structure also differs from corundum by a 180° rotation of every other octahedral sheet (along with a translation). The structural resemblance between corundum and Rh_2O_3 (II) suggests that their x-ray diffraction patterns should also be similar.

Pbnm-perovskite (Fig. 1D) represents another likely high pressure polymorph owing to the increased Al coordination (both six- and twelvefold), which provides added stability to cations at higher pressures (*20*). *Pbnm*-perovskite is the structure for $MgSiO_3$-perovskite (*21*), a major mineral phase in the Earth's mantle, with Mg and Si cations replacing the two Al cations of Al_2O_3. Such substitutions are common in minerals, suggesting that this structure may be possible for Al_2O_3 at high pressures. $R\bar{3}c$-perovskite (*22*) is found in some rare earth orthoaluminates

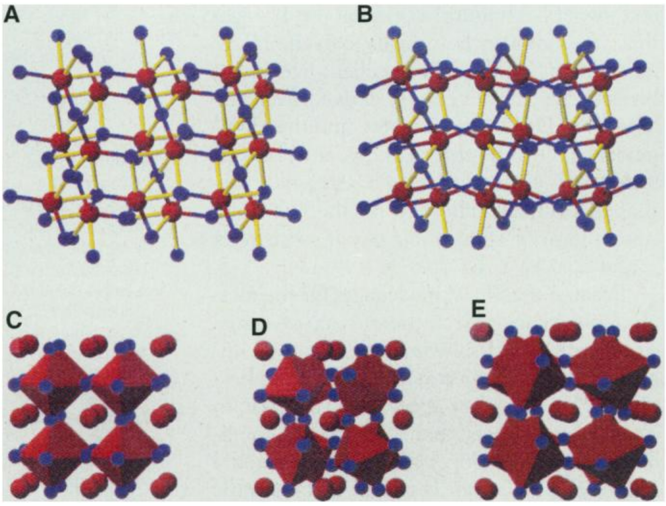

Fig. 1. Candidate structures of possible high pressure Al_2O_3 phases: (**A**) corundum, (**B**) Rh_2O_3 (II), (**C**) cubic-perovskite, (**D**) *Pbnm*-perovskite, and (**E**) $R\bar{3}c$-perovskite. Corundum has space group $R\bar{3}c$ with a rhombohedral unit cell containing 10 atoms (two Al_2O_3). The suspected high pressure polymorph, Rh_2O_3 (II), is related to corundum but its unit cell is orthorhombic, space group *Pbcn* with 20 atoms per cell (four Al_2O_3). *Pbnm*-perovskite represents another possible high-pressure phase and is shown as a distortion of the ideal cubic-perovskite structure in (C) and (D). The *Pbnm*-perovskite unit cell contains 20 atoms (four Al_2O_3). $R\bar{3}c$-perovskite has a rhombohedral unit cell containing 10 atoms (two Al_2O_3) and has the same space group as corundum. Aluminum atoms are represented as red spheres in (A) and (B) and as spheres and coordination polyhedra in (C), (D), and (E). The oxygen atoms are represented as blue spheres in all figures.

K. T. Thomson, Department of Chemical Engineering and Materials Science, and Minnesota Supercomputer Institute, University of Minnesota, Minneapolis, MN 55455, USA.
R. M. Wentzcovitch, Department of Chemical Engineering and Materials Science, and Minnesota Supercomputer Institute, University of Minnesota, Minneapolis, MN 55455, USA, and Instituto de Fisica, Universidade de Sao Paulo, CP 66318, 0 5389-970, Sao Paulo, SP, Brazil.
M. S. T. Bukowinski, Department of Geology and Geophysics, University of California, Berkeley, CA 94720, USA.

---

*To whom correspondence should be addressed.

Table 1. Zero pressure structural parameters for candidate structures of Al_2O_3. V_o, K, and K' are the calculated Birch-Murnaghan equation of state parameters including zero-pressure volume per Al_2O_3, bulk modulus, and first pressure derivative, respectively. Corundum and $R\bar{3}c$-perovskite lattice parameters: a_R, α, and c/a are based on a hexagonal unit cell while all others are given in terms of their orthorhombic unit cell. Internal positions for Al and O are reported for each structure in terms of their respective coordinate system. Cohesive energies are reported in units of electron volts per atom. Experimental values for corundum were obtained from (*34*) except cohesive energy, which was calculated from (*35*). Values in parentheses for corundum are calculated LAPW values from (*10*). Values in parentheses for Rh_2O_3 (II) and for *Pbnm*-perovskite are calculated values from (*8*) with the exception of V_o, K, and K' for Rh_2O_3 (II), which were calculated in (*10*). Lattice parameters are reported in atomic units (Bohr radii), and α is given in degrees.

	Corundum	Corundum (experiment)	Rh_2O_3 (II)	Pbnm perovskite	*$R\bar{3}c$ perovskite*
Group	*$R\bar{3}c$*		*Pbcn*	*Pbnm*	*R3c*
Z	2		4	4	2
V_o (au)	284.8 (282.1)	287.81	278.5 (275.6)	280.8 (302.4)	296.6
K (GPa)	258.9 (257)	254.4	261.8 (261)	235.0 (316)	216.0
K'	4.01 (4.01)	4.28	3.93 (3.97)	3.98 (4.11)	4.01
a_R (au)	9.661	9.705			9.678
alpha	55.41	55.286			56.77
c/a (hex.)	2.72	2.73			2.64
a			13.209 (13.26)	8.946 (8.91)	
b			9.056 (9.02)	9.190 (9.08)	
c			9.311 (9.20)	13.661 (13.72)	
$Al^{(1)}$	(0.352, 0.352, 0.352)	(0.352, 0.352, 0.352)	(0.110, 0.753, 0.032)	(0.510, 0.549, 0.250)	(0.250, 0.250, 0.250)
$Al^{(2)}$	—	—	—	(0.500, 0.000, 0.500)	(0.000, 0.000, 0.000)
$O^{(1)}$	(0.555, 0.945. 0.250)	(0.556, 0.944, 0.250)	(0.846, 0.607, 0.102)	(0.142, 0.412, 0.250)	(0.890, 0.610, 0.250)
$O^{(2)}$	—	—	(0.000, 0.049, 0.250)	(0.173, 0.176, 0.575)	—
E_c(eV)	7.34	6.33	7.26	7.19	7.12

(*23*) $MAlO_3$, where M = La, Pr, or Nd (Fig. 1E), and may also be a possible structural transformation for Al_2O_3 at high pressures.

We fit the calculated pressure-volume data for each structure to a third order Birch-Murnaghan (*24*) equation of state (Table 1), and the resulting bulk moduli and first order pressure derivatives of the moduli agreed with experimental data. Structural results were tested by comparing the zero-pressure lattice parameters and internal atomic coordinates of corundum to x-ray diffraction data; again the results were in agreement. At elevated pressures, the hexagonal unit cell of corundum exhibited a slight anisotropy with linear compressibilities of 1.22×10^{-3} and 1.39×10^{-3} GPa^{-1} along the *a* and *c* axis, respectively. These values compare favorably to experimental values (*25*).

Our low- to mid-pressure structural optimizations show that corundum transforms to Rh_2O_3 (II) at 78 ± 4 GPa (Fig. 2) accompanied by a 2.2% reduction in molar volume consistent with the reduction derived by (*10*). The observed anisotropy in linear compressibilities resulted in a 2.2% reduction in the *c/a* ratio of the corundum hexagonal unit cell at a pressure of 450 GPa compared to that of the zero pressure ratio. The internal positions of aluminum and oxygen also showed slight pressure depen-

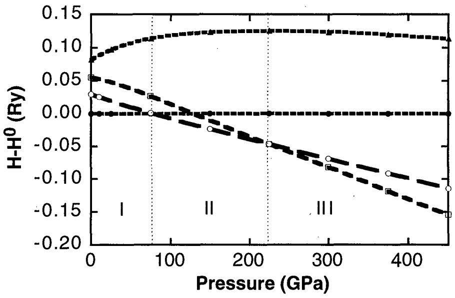

Fig. 2. Relative enthalpy versus pressure for high pressure Al_2O_3 candidate phases. Enthalpies are plotted relative to corundum (●) for pressures up to 450 GPa. Region I represents the pressure range where corundum is dominantly stable. The transition between regions I and II occurs at 78 ± 4 GPa where Rh_2O_3 (II) (○) overtakes corundum in stability. This transition is accompanied by a 2.2% reduction in volume and occurs at a volume ratio of V_T/V_o = 0.82 (relative to corundum at zero pressure). The transition to region III, where *Pbnm*-perovskite (■) becomes dominantly stable, occurs at 223 ± 10 GPa, accompanied by a 2.2% reduction in volume, and corresponds to a volume ratio of V_T/V_o = 0.68 (relative to Rh_2O_3 (II) at zero pressure). $R\bar{3}c$ = perovskite (▲) is also shown.

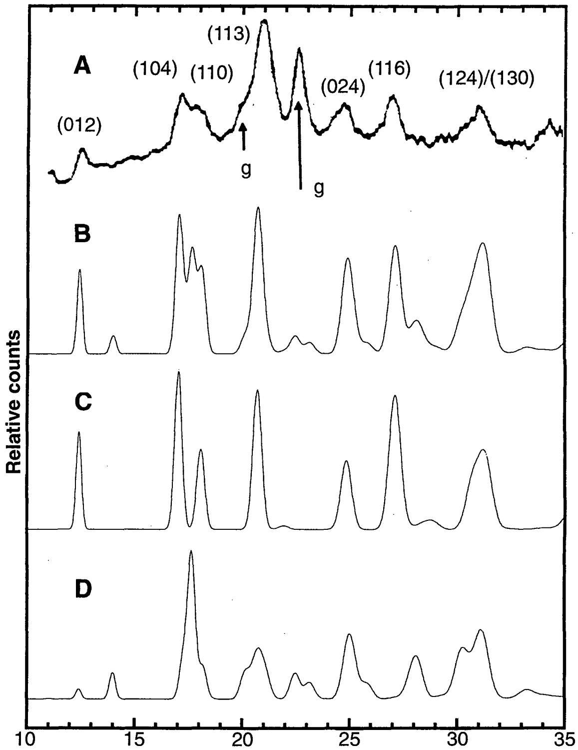

Fig. 3. Theoretical (*36*) and experimental energy-dispersive x-ray diffraction patterns for Al_2O_3. (**A**) Experimental Cr^{+3}-doped Al_2O_3 spectrum at 175 GPa (taken from Jephcoat *et al.* (*27*)). (**B**) Theoretical spectrum of a 50:50% mixture of Rh_2O_3 (II) and corundum at 175 GPa. (**C**) Theoretical spectrum of the pure corundum phase at 175 GPa. (**D**) Theoretical spectrum of the pure Rh_2O_3 (II) phase at 175 GPa. Weak diffraction from the sample confining gasket (iron) are represented by *g* as originally reported (*27*). All spectra intensities have been scaled for clarity.

dencies—a 0.6% and 1.4% variation, respectively. While small, these structural changes are energetically significant and constrain the predicted transition pressures. Our transition pressure was lower than the LAPW predicted value (*10*). The difference in calculated pressures may be caused by the full structural relaxations included in our calculations.

We observed an additional transformation to *Pbnm*-perovskite at 223 ± 15 GPa (with a 2.2% reduction of molar volume). Comparing the pressure dependence of enthalpy for each structure shows that while the perovskite is the second most energetic state at zero pressure, it is the most structurally adaptable to pressure increase. The *Pbnm*-perovskite structure has more degrees of freedom, and thus the enthalpies might be more affected by internal distortions. The distortion of the unit cell of the Al_2O_3-perovskite phase was similar to that of the $MgSiO_3$-perovskite phase at elevated pressures (*16*). This distortion causes both structures to become even more orthorhombic with increasing pressure (*26*).

Despite theoretical predictions that corundum should undergo two phase transitions, no experimental observations of such transformations have been observed in room temperature static compression of Al_2O_3 up to 175 GPa (*27*). High-temperature shock wave experiments suggest a possible density change at about 130 GPa (*28*) along with an enhanced thermal emission around 200 GPa (*29*), which nearly coincides with the pressure where the ruby fluorescence line appeared to vanish in static experiments (*5*) and where our predicted Rh_2O_3 (II) to *Pbnm*-perovskite transformation occurs. The vanishing of the ruby fluorescence line may be explained by diamond fluorescent emissions (*4*); however, this does not exclude the possibility of a concurrent transformation to *Pbnm*-perovskite.

The reconstructive nature of the predicted corundum to Rh_2O_3 (II) transition suggests that there may be a large hysteresis at the low temperatures typical of most diamond-anvil experiments (*4*, *30*, *31*). The lack of an observed corundum polymorph can thus be attributed to a metastable persistence of corundum beyond 78 GPa in static environments. However, it is also plausible that, because of the structural similarity between corundum and Rh_2O_3 (II) and the limited resolution of the x-ray diffraction at high pressures, the presence of Rh_2O_3 (II) has gone undetected (*27*).

A comparison of the calculated energy dispersive x-ray diffraction spectra for corundum and Rh_2O_3 (II) at 175 GPa illustrates this point (Fig. 3, C and D). Aside from a reduction in the number of shared coordination polyhedra edges, there is a loss of three-fold symmetry at the Al site in the transformation to Rh_2O_3 (II). These differences, along with a relative distortion of the AlO_6 polyhedra in Rh_2O_3 (II), are minor (Fig. 3). Therefore, even if Rh_2O_3 (II) were present in experiments, it is possible that it could not be detected.

Evidence for this hypothesis is provided by comparison of experimental diffraction data of Cr-doped corundum at 175 GPa by Jephcoat *et al.* (*27*) (Fig. 3A), with the calculated pattern of a 50:50% mixture of corundum and Rh_2O_3 (II) at the same pressure (Fig. 3B). The calculated pattern displays an extra line where the corundum (ϵ) and (ξ) lines are expected, and this triplet seems to match more closely the experimental spectrum in this region than the corundum spectrum does (Fig. 3C). It would be desirable to simultaneously raise the temperature in these experiments and examine the samples before and after quenching the pressure. High temperatures may provide the necessary kinetics for the transformation and residual amounts of the transformed phase may be observable at low pressures. Although it is standard practice not to heat the ruby pressure calibrant in diamond anvil cell experiments it remains unclear whether or not laser heating the sample may inadvertently affect the ruby pressure scale by allowing one of the proposed structural transformations to occur (*32*).

REFERENCES AND NOTES

1. R. H. Insley, in *Alumina Chemicals Science and Technology Handbook*, L. D. Hart, Ed. (American Chemical Society, Westerville, OH, 1990), p. 293.
2. W. J. Nellis and C. S. Yoo, *J. Geophys. Res.* **95**, 21749 (1990).
3. H.-K. Mao, J.-A. Xu, P. M. Bell, *ibid.* **91**, 4637 (1986).
4. J.-A. Xu, H.-K. Mao, P. M. Bell, *Science* **232**, 1404 (1986).
5. P. M. Bell, H.-K. Mao, K. A. Goettel, *ibid.* **226**, 542 (1984).
6. P. Richet, J.-A. Xu, H.-K. Mao, *Phys. Chem. Min.* **16**, 207 (1988).
7. R. E. Cohen, *Geophys. Res. Lett.* **14**, 37 (1987).
8. H. Cynn, D. G. Isaak, R. E. Cohen, M. F. Nicol, O. L. Anderson, *Am. Miner.* **75**, 439 (1990).
9. M. S. T. Bukowinski, A. Chizmeshya, G. H. Wolf, H. Zhang, *Mol. Eng.* **6**, 81 (1996).
10. F. C. Marton and R. E. Cohen, *Am. Miner.* **79**, 789 (1994). The authors derived a transition pressure of 86 ± 6 GPa for two **k**-points and 91 ± 6 GPa for ten **k**-points.
11. N. Troullier and J. L. Martins, *Phys. Rev. B* **43**, 1993 (1991). Our calculations were conducted using a plane wave cutoff energy E_{pw} of 70 Ry for wavefunctions (280 Ry for charge density and potential). Two irreducible **k**-points were used for the self-consistent potential calculation and total energy convergence was systematically tested with respect to E_{pw} and the number of **k**-points sampled. We performed minimizations for each structure at the pressure extremes (0 and 450 GPa) using four **k**-points. The resulting uncertainties (±4 GPa) in transition pressure are based on the interpolation of the transition pressure from the four **k**-point extrema and uncertainties in the two **k**-point calculations. Norm-conserving pseudo-potentials were generated using core cut-off radii of $r_s = r_p = 1.45$ au (atomic unit) (*p*-locality) and $r_s = r_p = r_d = 2.00$ au (*p*-locality) for oxygen and aluminum, respectively, and special care was taken to prevent core overlap at the highest pressures investigated (450 GPa).
12. R. M. Wentzcovitch, in *Quantum Theory of Real Materials*, J. R. Chelikowsky and S. G. Louie, Eds. (Kluwer Academic, Dordrecht, Netherlands, 1996), p. 113.
13. S. Lundqvist and N. H. March, *Theory of the Inhomogeneous Electron Gas* (Plenum, London, 1987).
14. D. M. Ceperley and B. J. Alder, *Phys. Rev. Lett.* **45** 566 (1981); J. P. Perdew and A. Zunger, *Phys. Rev. B* **23**, 5048 (1981).
15. R. M. Wentzcovitch, *Phys. Rev. B1* **44**, 2358 (1991).
16. ______, J. L. Martins, G. D. Price, *Phys. Rev. Lett.* **70**, 3947 (1993).
17. M. T. Yin and M. L. Cohen, *ibid.* **45**, 1004 (1980).
18. R. M. Wentzcovitch, N. L. Ross, D. G. Price, *Phys. Earth Planet. Int.* **90**, 101 (1995).
19. R. D. Shannon and C. T. Prewitt, *J. Solid State Chem.* **2**, 134 (1970).
20. C. W. F. T. Pistorius, *Prog. Solid State Chem.* **11**, 1 (1976).
21. R. Hemley and R. Cohen, *Ann. Rev. Earth Planet. Sci.* **20**, 553 (1992).
22. A. Glazer, *Acta Crystallogr.* **28**, 3384 (1972).
23. Derighetti *et al.*, *ibid.* **18**, 557 (1965); R. D. Burbank, *J. Appl. Cryst.* **3**, 112 (1970); M. Marezio, P. D. Dernier, J. P. Remeika, *J. Solid State Chem.* **4**, 11 (1972).
24. F. Birch, *J. Geophys. Res.* **83**, 1257 (1978).
25. L. W. Finger and R. M. Hazen, *J. Appl. Phys.* **49**, 5823 (1978).
26. In $MgSiO_3$ and Al_2O_3 perovskites, the *c/a* and *b/a* unit cell ratios increase with increasing pressure.
27. A. P. Jephcoat, R. J. Hemley, H. K. Mao, K. A. Goettel, *Physica B* **150**, 116 (1988).
28. J. S. Yu, *Appl. Sci. Res.* **19**, 220 (1968).
29. C. S. Yoo, N. C. Holmes, E. See, in *Shock Compression of Condensed Matter—1991*, S. Schmidt, R. D. Dick, J. W. Forbes, D. G. Pasker, Eds. (North-Holland, Amsterdam, 1992), pp. 733–736.
30. H. K. Mao, K. A. Goettel, P. M. Bell, in *Solid State Physics Under Pressure*, S. Minomura, Ed. (Terra, Tokyo, 1985), p. 11.
31. T. Gasparik, *Eos* **69**, 1451 (1988).
32. The ruby scale was calibrated against x-ray diffraction measurements of metal standards up to 180 GPa under non-hydrostatic conditions (*5*) and up to 110 GPa under quasihydrostatic conditions (*33*). Since our proposed transformation is within the above pressure range, in situ calibrations conducted at elevated pressures may have already taken into account any phase transformation that might have occurred.
33. R. J. Hemley *et al.*, *Phys. Rev. B* **39** 11827 (1989).
34. H. d'Amour, D. Schiferl, W. Denner, H. Schulz, W. B. Holzapfel, *J. Appl. Phys.* **49**, 4411 (1978).
35. *CRC Handbook of Chemistry and Physics*, R. C. Weast, Ed. (CRC Press, Boca Raton, FL, ed. 66, 1985).
36. The theoretical x-ray intensity patterns were generated from a superposition of Gaussian functions, centered on $2\theta(hkl)$, with half-widths $\sigma(hkl) = \sigma_o(1 + 2\theta(hkl)/140)$, where $\theta(hkl)$ is half the diffraction angle for *hkl* reciprocal lattice indices. This pattern was then converted to an energy dispersive pattern. The value of $\sigma_o = 2.0$ was chosen to give a peak width comparable to that of (*27*).
37. We thank R. Hemley for helpful comments on the manuscript. This research was supported by the Minnesota Supercomputer Center, the Center for Interfacial Engineering (an NSF Engineering Research Center) and through the National Science Foundation [awards EAR-9628199 (R.M.W.) and EAR-9526927 (M.S.T.B.)].

16 August 1996; accepted 11 October 1996